

## Protein-induced water $^1\text{H}$ MR frequency shifts: Contributions from magnetic susceptibility and exchange effects

Jie Luo<sup>a</sup>, Xiang He<sup>b</sup>, D. Andre' d'Avignon<sup>a</sup>, Joseph J.H. Ackerman<sup>a,b,c</sup>, Dmitriy A. Yablonskiy<sup>b,d,\*</sup>

<sup>a</sup> Department of Chemistry, Washington University, 1 Brookings Drive, Saint Louis, MO 63130, USA

<sup>b</sup> Department of Radiology, Washington University, 1 Brookings Drive, Saint Louis, MO 63130, USA

<sup>c</sup> Department of Internal Medicine, Washington University, 1 Brookings Drive, Saint Louis, MO 63130, USA

<sup>d</sup> Department of Physics, Washington University, 1 Brookings Drive, Saint Louis, MO 63130, USA

### ARTICLE INFO

#### Article history:

Received 13 August 2009

Revised 7 October 2009

Available online 30 October 2009

#### Keywords:

Susceptibility contrast

Water exchange

MRI

Phase imaging

BSA

1,4-Dioxane

TSP

### ABSTRACT

Defining the biophysics underlying the remarkable MRI phase contrast reported in high field MRI studies of human brain would lead to more quantitative image analysis and more informed pulse sequence development. Toward this end, the dependence of water  $^1\text{H}$  resonance frequency on protein concentration was investigated using bovine serum albumin (BSA) as a model system. Two distinct mechanisms were found to underlie a water  $^1\text{H}$  resonance frequency shift: (i) a protein-concentration-induced change in bulk magnetic susceptibility, causing a shift to lower frequency, and (ii) exchange of water between chemical-shift distinct environments, i.e., free (bulk water) and protein-associated ("bound") water, including freely exchangeable  $^1\text{H}$  sites on proteins, causing a shift to higher frequency. At 37 °C the amplitude of the exchange effect is roughly half that of the susceptibility effect.

© 2009 Elsevier Inc. All rights reserved.

### 1. Introduction

Gradient recalled echo (GRE) MR phase images acquired at high magnetic field strength show remarkably enhanced contrast between gray matter (GM) and white matter (WM) in human [1] and animal [2] brain. The contrast-to-noise ratio in MR phase images shows an almost 10-fold improvement over conventional MR magnitude images. Anatomic/functional structures that are not apparent on magnitude images can be visualized in phase images. Indeed, phase contrast has been explored for applications such as the study of multiple sclerosis [3] and Alzheimer's disease [4]. While the remarkable contrast observed at high field with phase imaging is provocative, the biophysical origins of this contrast are poorly understood. For example, phase variations have been observed across different brain regions [1], in both healthy and diseased brains. To fully quantify the anatomic, functional, and physiological information contained within phase images, it is crucial to understand the biophysical underpinnings of the MR "phase image" signal formation.

The MRI signal phase is determined by frequency shifts caused by multiple effectors. One group of effects relates to magnetic susceptibility variations within the tissue. Such tissue components as

lipids [1], non-heme iron [1,5–7], deoxyhemoglobin in the blood [1,8,9], and proteins [10,11] were suggested as possible sources of susceptibility variation. Importantly, He and Yablonskiy [12] showed that the MR signal frequency shift depends not only on tissue chemical composition but also on tissue architecture at the cellular and subcellular levels (i.e., geometrical distribution of cells and structures within the cells). They proposed a new theoretical concept for evaluation of the frequency shifts that lead to tissue phase contrast between GM/WM/CSF. Their theory provides a means to predict tissue frequency shifts from the known tissue architecture and magnetic susceptibilities of proteins, lipids, tissue iron and deoxyhemoglobin in the blood. The derived shifts agree very well with the experimental results of Duyn et al. [1]. Importantly, the work by He and Yablonskiy successfully explained the lack of phase contrast [1] between WM and CSF in the motor cortex area of the human brain.

However, another mechanism—the water-macromolecule exchange effect—has been suggested as an alternate or contributing cause of GM/WM phase image contrast [13]. The association of water and hydrophilic groups on the surface of macromolecules, including labile  $^1\text{H}$  sites, and resultant exchange between "bound" and "free" water, is known to substantially contribute to the water  $^1\text{H}$   $T_1$  and  $T_2$  relaxation times due to the abundant macromolecular content *in vivo*, especially proteins [14–18]. Although a water-macromolecule association/exchange mechanism cannot solely explain

\* Corresponding author. Fax: +1 314 362 0526.

E-mail address: [YablonskiyD@wustl.edu](mailto:YablonskiyD@wustl.edu) (D.A. Yablonskiy).

both the lack of contrast between CSF and WM [1] (protein contents are different: 10.9% in WM [19] and 0.015–0.045% in CSF [20]) and the orientation dependence of phase contrast in white matter [2], it remains important to assess the roles of exchange vs. susceptibility in the formation of phase contrast.

Proteins constitute one of the major components of brain tissue (~50% of dry tissue weight). Thus, it is reasonable to hypothesize that proteins could play a dual role—modulating both magnetic susceptibility and water-macromolecule exchange—in shifting the water MR frequency. Understanding the extent to which these roles are in play is important to quantitative interpretation of the contrast in GRE phase MR images. Hence, the major goal of this manuscript is to separate and scale the contributions of protein-induced magnetic susceptibility and exchange effects to the observed shifts in MR signal frequency.

## 2. Materials and methods

An aqueous solution of BSA (bovine serum albumin) was chosen as a model system to study the effects of protein content on the water  $^1\text{H}$  MR signal frequency. 1,4-Dioxane (“Dioxane”), which has been reported to be an appropriate internal reference in protein solutions [21], was employed as an internal  $^1\text{H}$  MR frequency reference.

### 2.1. Sample preparation

To prepare a stock protein solution, 10 g BSA (99% purity, Sigma, [CAS No. 9048-46-8]) was dissolved in de-ionized water (with 0.5% v/v Dioxane) to a final volume 100 ml. The solution was clear to the eye, indicating the lack of residual insoluble components. Additional BSA samples were prepared from this stock solution by dilution with de-ionized water (which also contained 0.5% v/v Dioxane) to concentrations of 25, 50, 75, 100 mg (BSA)/ml (solution). The BSA volume fraction of the stock solution was calculated by weighing the volumetric flask before and after making the solution; from the mass of the BSA powder and the mass of the total solution, the mass of de-ionized water was determined. Knowing the density of water at the relevant temperature, the water and BSA volume fractions were derived.

### 2.2. Mechanisms affecting the $^1\text{H}$ water MR signal frequency

The magnetic resonance frequency  $f$  of a spin immersed in a homogeneous media containing macromolecules can be described by several additive components: (i) a component  $f_0 = \gamma \cdot B_0$ , the base Larmor resonance frequency, where  $\gamma$  is the gyromagnetic ratio and  $B_0$  is the main static field, (cgs units are used throughout this paper), (ii) a component  $\Delta f_\chi$  due to the magnetic susceptibility of the media, (iii) a component  $\Delta f_e$  due to chemical exchange between free (bulk) water and bound water, typically that associated with hydrophilic groups on the surface (and perhaps interior) of macromolecules, and (iv) a component  $-\sigma f_0$  due to the local, electronic shielding provided by the “host” water molecule (shielding factor  $\sigma$ ):

$$f = f_0 + \Delta f_\chi + \Delta f_e - \sigma \cdot f_0. \quad (1)$$

The frequency component  $\Delta f_\chi$  due to magnetic susceptibility for a homogeneous, isotropic liquid (media) can be described as a sum of two terms. The first term arises from the presence of the media's external boundary:

$$\Delta f/f_0 = A \cdot \chi, \quad (2)$$

where  $\chi$  is the volume magnetic susceptibility of the media. Here for simplicity we only consider media whose boundary can be

described by an arbitrary ellipsoidal shape. Hence, the magnetic field inside the boundary containing the media is homogeneous with the factor  $A$  depending on the specific shape of the media boundary (see the discussion in [22]). For example, if the media boundary forms an infinitely long cylinder, oriented with angle  $\theta$  between the cylinder's main axis and  $B_0$ ,  $A = -2\pi \cdot \sin^2 \theta$ , while for a spherical boundary  $A = -\frac{4}{3}\pi$ . The second term describes the frequency shift caused by neighboring molecules, which in the Lorentzian sphere approximation can be represented as:

$$\Delta f/f_0 = \frac{4\pi}{3} \cdot \chi. \quad (3)$$

The concept embodied in the Lorentzian sphere approximation has played an important role in the evaluation of magnetic susceptibility effects on the MR frequency shift  $\Delta f$ . It is based on the assumption that for a homogeneous, isotropic solution the microscopic local field acting on a spin can be evaluated as if this spin were moving inside a hollow sphere embedded in the magnetized media, while the media outside the Lorentz sphere can be modeled as a homogeneous and isotropic continuum. With these assumptions, the frequency shift  $\Delta f$  in the presence of external static field  $B_0$  is described by Eq. (3). It should be noted, however, that in biological tissues exhibiting anisotropic structure (i.e., white matter in the brain), the Lorentzian sphere approximation is no longer valid and a more general approach should be used [12].

### 2.3. Measurement of the magnetic susceptibility of BSA

A scheme employing orthogonal tubes was applied to measure the volume magnetic susceptibility of the BSA solutions [22]. Standard, 5 mm diameter, 7" long, glass “NMR tubes” were filled with degassed BSA solutions and sealed with parafilm. A given tube was first oriented parallel to the magnetic field and then perpendicular to the field. Under these conditions, the MR signal frequency difference between the two orthogonal orientations will be determined only by the susceptibility effects created by the boundary of the tube (coefficient  $A$  in Eq. (2)). Any other factors remain constant and, thus, are cancelled out.

During the experiment, since the tube is positioned in air instead of a vacuum, the frequency difference between the two orientations will be (the same for both water and Dioxane):

$$\Delta f = 2\pi \cdot (\chi_{\text{solution}} - \chi_{\text{air}}) \cdot \gamma \cdot B_0, \quad (4)$$

where

$$\chi_{\text{solution}} = \chi_{\text{water}} + \zeta_{\text{protein}} \cdot (\chi_{\text{protein}} - \chi_{\text{water}}) + \zeta_{\text{Dioxane}} \cdot (\chi_{\text{Dioxane}} - \chi_{\text{water}}) \quad (5)$$

and  $\zeta$  indicates the relevant solution-component volume fraction. Thus, by measuring  $\Delta f$  at different volume fractions of BSA ( $\zeta_{\text{protein}}$ ), the volume magnetic susceptibility difference between BSA and water ( $\chi_{\text{protein}} - \chi_{\text{water}}$ ) can be determined. Further, since  $\chi_{\text{water}}$  is a known parameter, the volume magnetic susceptibility of BSA can be determined.

Susceptibility measurement experiments were performed on a Varian DirectDrive™ MR scanner based on a 4.7T horizontal-bore superconducting magnet with a 21 cm-bore inner-diameter gradient and shim assembly using a 1.5 cm diameter, laboratory constructed, surface transmit/receive RF coil. A PRESS sequence was employed for localized shimming and data acquisition from a  $4 \times 4 \times 4 \text{ mm}^3$  voxel selected at the mid point of the cylinder's axial length. Forty minutes prior to initiating experiments, a thermometer and all the tubes to be scanned were positioned at one end of the magnet for temperature stabilization. As noted above, each sample tube was first oriented parallel to the magnetic field  $B_0$  and shimming was performed on the selected voxel. The  $^1\text{H}$

resonance frequencies of water and Dioxane were measured. Then, immediately following data acquisition, the tube was carefully rotated about the voxel position so as to align it perpendicular to the magnetic field and the signal frequencies were determined again. For both orientations, the shim settings (currents in the shim coils) and the voxel positioning were kept the same. At each orientation, thirty individual (not summed) free induction decays were acquired with 4000 Hz bandwidth, 3 s data sampling period, and 10 s TR.

Frequencies for both water and Dioxane  $^1\text{H}$  resonances were determined separately for each of the 30 individual spectra using Bayesian probability analysis [23]. During the 5 min total acquisition time, the water frequency drifted about 0.022 ppm while the Dioxane frequency fluctuated around a mean  $\pm$  SD of  $7.1187 \pm 0.0002$  ppm, indicating that field drift was minimal. The water frequency drift was presumably reflective of a  $\sim 2$  K temperature decrease ( $\sim -0.011$  ppm/K) [24], associated with relocating the sample to the observation coil. If any untoward field/frequency shift was detected during the experiment, e.g., if a light rail train passed by the scanner site (the scanner is  $\sim 150'$  feet distant from the train track), the experiment was repeated. The  $^1\text{H}$  resonance frequency of Dioxane (the mean of all 30 individually analyzed data sets) was used to determine the frequency differences between orthogonal orientations of the same sample contained in a given tube.

#### 2.4. Separation of magnetic susceptibility and exchange effects

To separate susceptibility and exchange effects, a scheme employing coaxial tubes was employed. The inner tube (2 mm outer diameter) was filled with aqueous solutions containing different concentrations of BSA, including 0.5% Dioxane; the outer tube (5 mm outer diameter) was filled with water (no BSA) and 0.5% Dioxane. Accordingly, the magnetic susceptibility of the BSA solution in the inner tube was defined by Eq. (5), and the magnetic susceptibility of the reference solution (no BSA) in the outer tube is:

$$\chi_{\text{ref}} = (1 - \zeta_{\text{Dioxane}}) \cdot \chi_{\text{water}} + \zeta_{\text{Dioxane}} \cdot \chi_{\text{Dioxane}}. \quad (6)$$

Since the orientation factor  $A$  in Eq. (2) nulls when both coaxial compartments are parallel to the  $B_0$  field, the  $^1\text{H}$  MR signal frequency shift induced by the susceptibility difference between inner and outer tubes is:

$$\Delta f/f_0 = \frac{4\pi}{3} \cdot (\chi_{\text{inner}} - \chi_{\text{outer}}) = \frac{4\pi}{3} \cdot \zeta_{\text{protein}} \cdot (\chi_{\text{protein}} - \chi_{\text{water}}) \quad (7)$$

Dioxane is not expected to undergo exchange or physically/chemically associate with BSA molecules. Thus, the frequency difference of Dioxane resonances between inner and outer tubes is taken to reflect a pure susceptibility effect per Eq. (7). However the water frequency difference between inner and outer tubes reflects both the protein induced susceptibility and exchange effects:

$$\Delta f_{\text{water}}/f_0 = \Delta f_e + \frac{4\pi}{3} \cdot (\chi_{\text{inner}} - \chi_{\text{outer}}). \quad (8)$$

Note that  $\Delta f_e$  is also proportional to the volume fraction of BSA. Therefore, by subtracting the frequency shift of Dioxane from the frequency shift of water, the net frequency shift due to water–BSA exchange can be quantified.

The coaxial tubes MR experiment was conducted on a Varian Inova 500 MHz (11.74 T) vertical bore high resolution spectrometer. The probe was equipped with a variable temperature controller and all samples were stabilized at a fixed temperature before and during the measurement. Data was acquired at two temperatures: 286.5 K (same as with the 4.7 T imaging scanner) and 310 K (similar to body temperature). Samples did not contain  $\text{D}_2\text{O}$ , commonly used for field/frequency locking and shimming. A separate coaxial

tube containing a  $\text{D}_2\text{O}/\text{H}_2\text{O}$  mixture was used for shimming. After shimming, thirty individual free induction decays were collected on each of the relevant coaxial samples, with 10,000 Hz bandwidth, 2 s acquisition time, and 10 s TR. Radiation damping was eliminated by detuning the receiver coil and employing a reduced filling factor (5 mm outer tube diameter in a RF coil greater than 10 mm in diameter).

Because data were acquired without a field/frequency lock, and there was not enough SNR for accurate evaluation of the Dioxane frequency in the inner tube from a single acquisition, the following procedure was used to correct for field drift. In each data set composed of 30 individual FIDs, the first FID acquired was used as a reference; the frequency shift caused by field drift was calculated by comparing the phase of the water signal in each of the 29 subsequent FIDs to the reference FID. The time domain data from each individual acquisition were then frequency shifted correspondingly and averaged (sum of 30 FIDs) after this correction. The frequencies of each resonance (water and Dioxane) in the coaxial tubes were determined from the summed FIDs for different protein concentrations using Bayesian probability analysis [23].

### 3. Results

Examples of water and Dioxane spectra obtained in an orthogonal tubes experiment and a coaxial tubes experiment are shown in Fig. 1a and b. Double peaks for water and Dioxane can be observed for the coaxial tubes experiment. These peaks correspond to water and Dioxane in the outer (large amplitude signals) and inner tube (small amplitude signals) compartments.

Fig. 2 illustrates the observed frequency difference in the orthogonal tubes experiment at different protein concentrations. Fitting Eq. (4) to the  $\Delta f_{\text{solution}}$  vs. volume fraction of BSA data yields (mean  $\pm$  SD):  $\chi_{\text{protein}} - \chi_{\text{water}} = (-0.107 \pm 0.009)$  ppm and  $\chi_{\text{water}} - \chi_{\text{air}} + \zeta_{\text{Dioxane}} \cdot (\chi_{\text{Dioxane}} - \chi_{\text{water}}) = -(0.7513 \pm 5\text{E}-4)$  ppm. Given the susceptibility of water ( $-0.719$  ppm [25]), the estimated volume magnetic susceptibility of BSA can be derived:

$$\chi_{\text{BSA}} = (-0.826 \pm 0.009) \text{ ppm}. \quad (9)$$

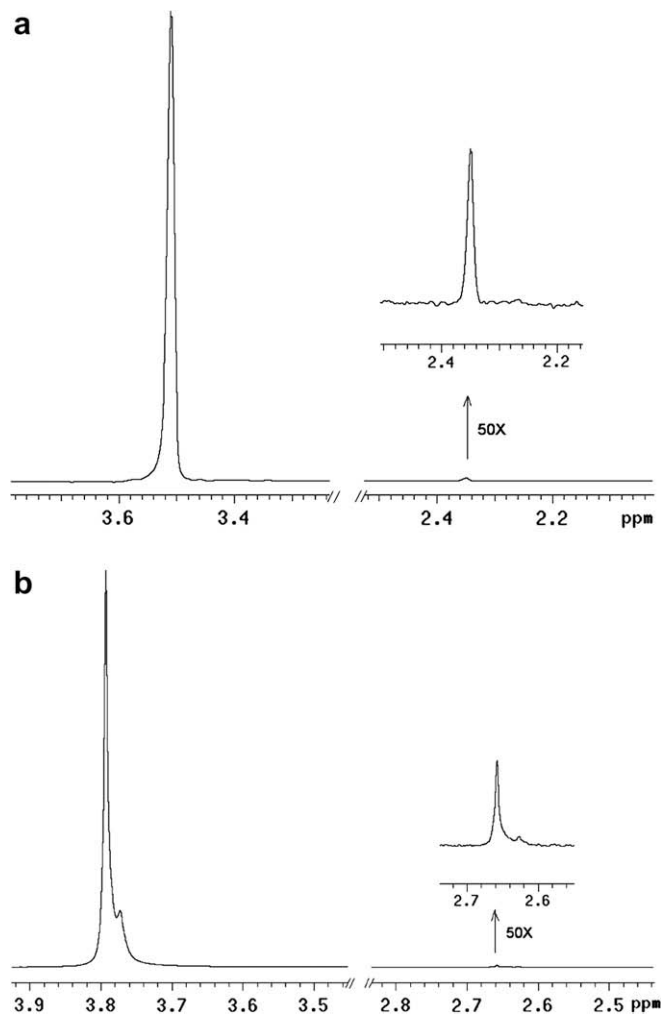
Further, given  $\chi_{\text{Dioxane}} = -0.596$  ppm [25], the magnetic susceptibility of air can be derived,  $\chi_{\text{air}} = (0.0317 \pm 5\text{E}-4)$  ppm. The positive magnetic susceptibility of air is caused by the presence of  $\text{O}_2$ , which is paramagnetic. This result is in excellent agreement with the susceptibility of oxygen in air as estimated from first principles using the Curie law,  $\chi_{\text{oxygen}} = 0.0316$  ppm, given the known molar magnetic susceptibility of pure  $\text{O}_2$  ( $\chi_m(\text{O}_2) = 3372$  ppm  $\text{cm}^3 \text{mol}^{-1}$  at 13 °C [25]) and its volume fraction in air (21%). While this effect is small, it should be taken into account for accurate measurements of magnetic susceptibility.

Fig. 3 shows the  $^1\text{H}$  MR signal frequency difference between inner and outer tubes for water and Dioxane in the coaxial tubes experiment at two temperatures. Note that the  $^1\text{H}$  frequency shift of water is the sum of the magnetic susceptibility effect and the water–exchange effect. Since Dioxane does not associate with BSA (*vide infra*), the frequency shift of Dioxane can be attributed solely to a susceptibility effect:

$$\Delta f/f_0|_{\text{susceptibility}} = \Delta f/f_0|_{\text{Dioxane}} = -(0.45 \pm 0.03) \cdot \zeta \text{ ppm}. \quad (10)$$

As calibrated by Dioxane's pure susceptibility induced frequency shift, a BSA induced susceptibility effect will decrease the water  $^1\text{H}$  resonance frequency. This is in agreement with our previous orthogonal tubes measurement.

Having quantified the magnetic susceptibility effect, the contribution of water–BSA exchange to the water MR signal frequency shift can be estimated by subtracting susceptibility frequency shifts from the observed water frequency shifts:



**Fig. 1.** Examples of spectra (line-broadening apodization filter of 1 Hz) obtained from the orthogonal tubes experiment (a), and the coaxial tubes experiment after averaging (b). The Dioxane resonances are shown vertically expanded (50 $\times$ ) in the insets. Both experiments were carried out at the same temperature (286.5 K) and the protein solutions in both experiments contained 7.5% (v/v) BSA and 0.5% Dioxane. Resonance frequencies were determined by Bayesian probability analysis [23]. Estimated uncertainties of resonance frequencies in (a) are:  $1.3E-5$  ppm for water and  $2.5E-4$  ppm for Dioxane. Estimated uncertainties of resonance frequencies in (b) are: outer-tube water  $1E-5$  ppm, inner-tube water  $3.9E-5$  ppm, outer-tube Dioxane  $9.7E-5$  ppm, inner-tube Dioxane  $1E-3$  ppm.

$$\begin{aligned} \text{at } 13.5^\circ\text{C}: \Delta f/f_0|_{\text{exchange}} &= \Delta f/f_0|_{\text{water}} - \Delta f/f_0|_{\text{susceptibility}} \\ &= (0.17 \pm 0.03) \cdot \zeta \text{ ppm}, \end{aligned} \quad (11)$$

$$\begin{aligned} \text{at } 37.0^\circ\text{C}: \Delta f/f_0|_{\text{exchange}} &= \Delta f/f_0|_{\text{water}} - \Delta f/f_0|_{\text{susceptibility}} \\ &= (0.23 \pm 0.03) \cdot \zeta \text{ ppm}. \end{aligned} \quad (12)$$

Hence, water exchange/association with BSA increases linearly with protein concentration as would be expected. It results in a frequency shift in opposite direction to that caused by protein susceptibility.

#### 4. Discussion

This work examines the homogenous model system of a native protein in solution. Two mechanisms through which proteins affect the water  $^1\text{H}$  MR signal frequency are considered: magnetic susceptibility and water–protein exchange/association. The magnetic susceptibility of a substance is related to the electronic structure of its atoms. Protein density (g/ml) is greater than that

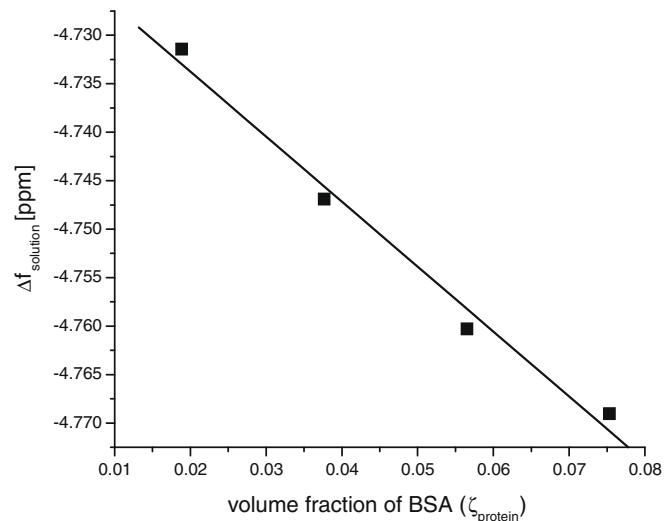


**Fig. 2.** The dependence of magnetic susceptibility induced MR signal frequency shifts on protein volume fractions.  $\Delta f_{\text{solution}}$  is the Dioxane MR signal frequency difference between cylindrical NMR tube orientations parallel and perpendicular to  $B_0$  in the rotating tube experiment.

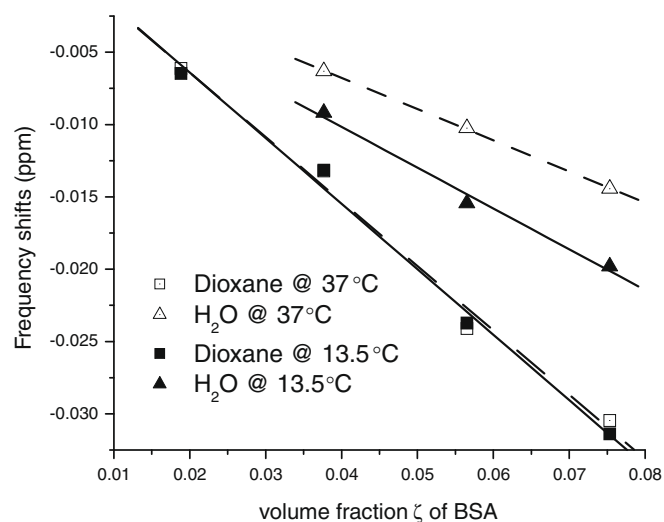


**Fig. 3.**  $^1\text{H}$  MR signal frequency difference of water (triangles) and Dioxane (squares) between inner and outer coaxial tubes  $(f_{\text{inner}} - f_{\text{outer}})/f_0$  measured at  $13.5^\circ\text{C}$  (solid symbols) and  $37^\circ\text{C}$  (open symbols). Lines represent linear regressions. The slopes of the fitted lines are:  $(-0.45 \pm 0.03)$  [ppm] for Dioxane, and  $(-0.28 \pm 0.03)$  [ppm] for water at  $13.5^\circ\text{C}$ ;  $(-0.445 \pm 0.03)$  [ppm] for Dioxane and  $(-0.216 \pm 0.004)$  [ppm] for water at  $37^\circ\text{C}$ .

of water. The presence of proteins in aqueous solution increases the density of circulating electrons (within molecular orbitals), thus making the solution more diamagnetic. (Recall, diamagnetism is related to changes in the molecular electron currents induced by the magnetic field.) According to Eq. (10) this decreases the water  $^1\text{H}$  MR signal frequency. Water–protein exchange can be envisaged as a rapidly time modulated interaction/association between water and multiple exchangeable sites on protein residues (primarily  $-\text{NH}-$ ,  $-\text{NH}_2$ ,  $-\text{OH}$ ,  $-\text{SH}$  and  $-\text{COOH}$ ). The overall effect is a shift of the water  $^1\text{H}$  MR signal to higher frequencies. On a protein volume fraction basis, the susceptibility effect is twice that of, and in opposition to, the exchange effect. As shown in Fig. 3, the susceptibility induced frequency shift is not affected by temperature (as expected because small temperature variations have little effect on molecular electronic structure), while the exchange induced frequency shift is affected by temperature. This is also expected be-

cause temperature influences the rates of kinetic processes including protein conformational dynamics, which consequently alters exchange/association phenomena between water and protein [26].

As noted above, in native BSA solution at 37 °C the amplitude of the exchange effect is one half and opposite in sign to that of the susceptibility effect. It is likely the water–protein exchange effect is even smaller in biological tissues where proteins are often cross-linked, associated with membranes or other proteins and sites for water association are reduced in number. Indeed, as a globular protein, BSA has a hydrophobic core and a hydrophilic surface, which makes it soluble in water. Its structure is representative for a large group of proteins: hemoglobulins, immunoglobulins, albumins, enzymes, etc. Considering brain *in vivo*, apart from the soluble proteins, the other major protein class is insoluble in water [27–29], namely, fibrous proteins (scleroproteins), which form neurofilaments and microtubules, etc. These proteins are found as aggregates due to hydrophobic groups that stick out of the molecules, providing mechanical strength and rigidity for the tissue as well as for physiological functions. Due to their aggregated structural features, protons on the surface of fibrous proteins are more likely to have very short  $^1\text{H}$   $T_2$  relaxation time constants, further resulting in a reduction of water frequency shifts due to exchange effects. Hence, comparing with the model native protein solution employed herein, it is likely exchange effects *in vivo* will contribute even less to the water MR signal frequency shift. At the same time, protein contribution *in vivo* to tissue magnetic susceptibility will remain the same as measured herein. (The reader is reminded that the contribution of highly anisotropically organized protein structures to the water  $^1\text{H}$  MR signal frequency shift can not be described in terms of the Lorentzian sphere approximation, Eq. (3), a more general approach must be applied [12].)

This method employed herein for separating magnetic susceptibility and exchange effects relies on having a reliable internal reference, Dioxane, that does not interact/associate with BSA. Several lines of evidence support the choice of Dioxane for this purpose. First, the Dioxane  $^1\text{H}$  MR signal in the compartment with BSA showed no line broadening, consistent with a lack of significant interaction/association between Dioxane and BSA. Second, measurements of Dioxane frequency shift vs. protein concentration at 13.5 °C and 37 °C (see Fig. 3) showed no temperature dependence, again consistent with a lack of significant interaction/association between Dioxane and BSA (as was not the case for water, Fig. 3). Third, comparison of results obtained in the orthogonal tubes experiment with those from the coaxial tubes experiment further confirms that Dioxane exhibits no (or negligible) interaction/association with BSA. Indeed, we have determined from the orthogonal tubes experiment that the magnetic susceptibility of BSA is  $\chi_{\text{BSA}} = (-0.826 \pm 0.009)$  ppm, see Eq. (9). Substituting this value into Eq. (7) we can predict that the frequency shift of the Dioxane MR signal between inner and outer compartments in the coaxial tubes experiment should be  $(\Delta f/f_0)_{\text{Dioxane}} = -(0.45 \pm 0.04) \cdot \zeta$  ppm. This follows only if the frequency shift of the Dioxane signal is solely due to the magnetic susceptibility effect. Direct measurement as described in Eq. (10) is in an excellent agreement with this prediction. That is, the frequency shift of Dioxane between inner and outer tubes is not affected by exchange/association with BSA, and reflects a pure susceptibility effect.

Although some studies suggest that Dioxane and water could affect each other's frequencies by 'bifunctional hydrogen bonds' [30], the absolute frequencies of Dioxane and water are not important in these measurement. Further, the same Dioxane concentration is maintained in both inner and outer coaxial tubes, thus the frequency difference between the two coaxial tubes is due solely to protein content.

These quantitative results regarding volume susceptibility are reported with respect to the volume fraction of BSA, which was cal-

culated based on directly weighing protein powder and the measurement of solution volume. The estimated protein density in our solution was 1.332 g/cc, which is lower than the density of fully "dry" serum albumin reported as 1.381 g/cc [31]. It is known, however, that crystalline protein is likely to contain approximately 10% (w/w) of water [32]. Hence, from the density difference we can estimate that the water content in our purchased BSA is 10.6% (w/w)—similar to previously reported. Accordingly, we can recalculate the volume susceptibility of "pure" BSA as  $\chi(\text{pure BSA}) = -0.841$  ppm and the gram susceptibility as

$$\chi_g(\text{pure BSA}) = -0.609 \text{ ppm}[\text{ml/g}], \quad (13)$$

which is in good agreement with previously reported "common  $\chi_g$  value" of proteins:  $-(0.587 \pm 0.005) \times 10^{-6} \text{ ml/g}$  [33]. Using the corrected value, we can re-examine the contribution of "pure" proteins to the water MR signal frequency shift at 37 °C:

$$\begin{aligned} \Delta f/f_0|_{\text{susceptibility}} &= -0.51 \cdot \zeta_{\text{pure}} \text{ ppm} \\ \Delta f/f_0|_{\text{exchange}} &= 0.26 \cdot \zeta_{\text{pure}} \text{ ppm} \end{aligned} \quad (14)$$

The possible role of water–protein exchange effects in the formation of  $^1\text{H}$  water MR signal frequency shifts was first addressed by Zhong et al. [13]. Data presented herein are different from their results, which utilized TSP as an internal reference. While TSP is broadly used in high resolution  $^1\text{H}$  NMR experiments, our experimental data (see Appendix A) suggests that TSP exhibits significant interaction with BSA. The line width of TSP in the coaxial tube with BSA is largely broadened compared to the line width of TSP in the coaxial tube without BSA. The frequency shift of TSP between the two coaxial tubes per unit volume BSA ( $-1.03 \pm 0.07$  ppm) does not match the susceptibility effect determined by our orthogonal tube experiment ( $-0.45 \pm 0.04$  ppm), indicating the TSP frequency shift results from more than just the susceptibility effect of BSA. It is well known that an important function of serum albumin is to bind long-chain fatty acids and other like molecules, serving as a major transporter for free fatty acids *via* the plasma [34,35]. Although the TSP is only equivalent to a 5-carbon chain, it is possible that BSA weakly binds with TSP, resulting in a certain degree of exchange driven frequency shift. Earlier studies have reported that the chemical shift of TSP was dependent on the protein concentration [21].

## 5. Conclusion

In this study, the effects of protein content on water  $^1\text{H}$  frequency shifts were examined. These shifts will contribute to the phase shift *in vivo* at high field. Two previously suggested mechanisms were determined separately and quantitatively by an experiment employing coaxial tubes and native protein (BSA) solutions. Results indicate that the protein susceptibility effect is twice that of, and in opposite direction to, the exchange effect. Excellent agreement between protein susceptibility measurement employing coaxial tubes and measurement employing an orthogonal tube protocol confirmed that Dioxane is a reliable marker for separation of magnetic susceptibility and exchange effects. This is further supported by a frequency shift, temperature dependence study. These experimental findings with native protein solution provide insights into the influence of protein content on water  $^1\text{H}$  MR signal frequency. For structurally cross-linked proteins *in vivo*, the susceptibility effect is expected to play an even more substantial role in affecting the water  $^1\text{H}$  MR frequency.

## Acknowledgements

This work is supported by grants ROI-NS055963 and R24-CA83060. The authors are grateful to Drs. Oliver Speck and Kai Zhong for helpful discussions.

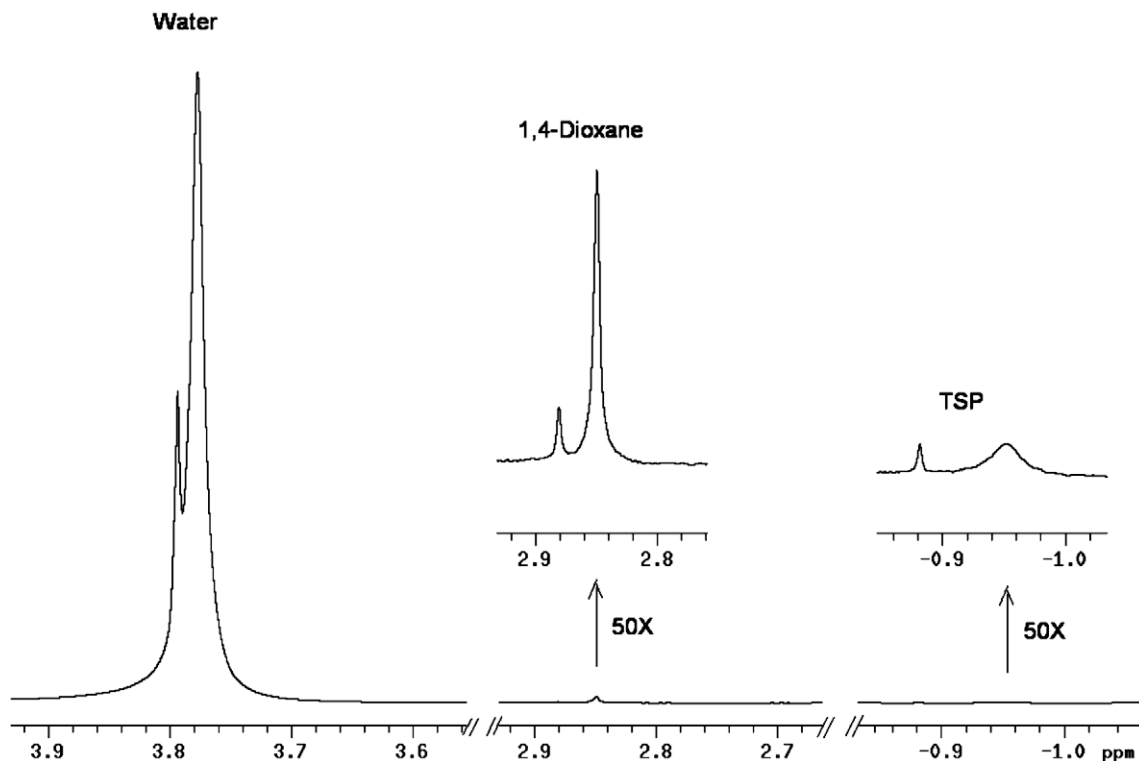


**Fig. 4.** A significantly broadened TSP resonance in the presence of BSA. Line broadening is not observed for the Dioxane resonance. With regard to the frequency shifts at this particular protein concentration: TSP is shifted by  $-0.072$  ppm whereas Dioxane is shifted by  $-0.031$  ppm. If TSP is taken as an internal reference and the BSA exchange effect on signal frequency is calculated, it would be  $+0.055$  ppm instead of  $+0.015$  ppm (using Dioxane as reference), a substantial systematic error.

## Appendix A

TSP (2,2,3,3-tetradeuterio-3-trimethylsilyl-propionate, 0.5% (w/w), 29 mM) powder was added to the BSA stock solution and a control solution without BSA. The same experiment employing coaxial tubes as described in the main text was conducted to compare the TSP  $^1\text{H}$  MR signal frequency change with that of Dioxane. However, the BSA solution was placed in the outer tube for improved detection (TSP has a broad line width in the presence of BSA).

Fig. 4, spectrum (line-broadening apodization filter = 1 Hz) from experiment employing coaxial tubes. Concentric tubes were positioned parallel to the  $B_0$  field, with temperature stabilized at  $37^\circ\text{C}$ . The solution in the outer tube contained 7.5% (v/v) BSA, 0.5% Dioxane, and 0.5% (w/w) TSP; the solution in the inner tube contained 0.5% Dioxane and 0.5% (w/w) TSP. Dioxane and TSP resonances are vertically expanded ( $50\times$ ) in the insets.

## References

- [1] J.H. Duyn, P. van Gelderen, T.Q. Li, J.A. de Zwart, A.P. Koretsky, M. Fukunaga, High-field MRI of brain cortical substructure based on signal phase, *Proc. Natl. Acad. Sci. USA* 104 (2007) 11796–11801.
- [2] J.P. Marques, R. Maddage, V. Mlynarik, R. Gruetter, On the origin of the MR image phase contrast: an in vivo MR microscopy study of the rat brain at 14.1 t, *Neuroimage* 46 (2009) 345–352.
- [3] K.E. Hammond, M. Metcalf, D.T. Okuda, S.J. Nelson, D.B. Vigneron, D. Pelletier, In vivo high resolution MR imaging at 7t of multiple sclerosis with sensitivity to iron, *Neurology* 70 (2008) A8.
- [4] B. Ding, K.M. Chen, H.W. Ling, F. Sun, X. Li, T. Wan, W.M. Chai, H. Zhang, Y. Zhan, Y.J. Guan, Correlation of iron in the hippocampus with mmse in patients with alzheimer's disease, *J. Magn. Reson. Imaging* 29 (2009) 793–798.
- [5] E.M. Haacke, N.Y. Cheng, M.J. House, Q. Liu, J. Neelavalli, R.J. Ogg, A. Khan, M. Ayaz, W. Kirsch, A. Obenaus, Imaging iron stores in the brain using magnetic resonance imaging, *Magn. Reson. Imaging* 23 (2005) 1–25.
- [6] J.F. Schenck, E.A. Zimmerman, High-field magnetic resonance imaging of brain iron: birth of a biomarker?, *NMR in Biomed* 17 (2004) 433–445.
- [7] J.F. Schenck, Magnetic resonance imaging of brain iron, *J. Neurol. Sci.* 207 (2003) 99–102.
- [8] D.A. Yablonskiy, E.M. Haacke, Theory of nmr signal behavior in magnetically inhomogeneous tissues: the static dephasing regime, *Magn. Reson. Med.* 32 (1994) 749–763.
- [9] B. Yao, T.Q. Li, P. van Gelderen, K. Shmueli, J.A. de Zwart, J.H. Duyn, Susceptibility contrast in high field MRI of human brain as a function of tissue iron content, *Neuroimage* 44 (2009) 1259–1266.
- [10] W.M. Spees, D.A. Yablonskiy, M.C. Oswood, J.J. Ackerman, Water proton MR properties of human blood at 1.5 tesla: magnetic susceptibility,  $t(1)$ ,  $t(2)$ ,  $t^*(2)$ , and non-lorentzian signal behavior, *Magn. Reson. Med.* 45 (2001) 533–542.
- [11] X. He, M. Zhu, D.A. Yablonskiy, Validation of oxygen extraction fraction measurement by qbold technique, *Magn. Reson. Med.* 60 (2008) 882–888.
- [12] X. He, D.A. Yablonskiy, Biophysical mechanisms of phase contrast in gradient echo MRI, *Proc. Natl. Acad. Sci. USA* 106 (2009) 13558–13563.
- [13] K. Zhong, J. Leupold, D. von Elverfeldt, O. Speck, The molecular basis for gray and white matter contrast in phase imaging, *Neuroimage* 40 (2008) 1561–1566.
- [14] R.G. Bryant, The dynamics of water–protein interactions, *Annu. Rev. Biophys. Biomol. Struct.* 25 (1996) 29–53.
- [15] H.I. Mäkelä, O.H.J. Gröhn, M.I. Kettunen, R.A. Kauppinen, Proton exchange as a relaxation mechanism for T1 in the rotating frame in native and immobilized protein solutions, *Biochem. Biophys. Res. Commun.* 289 (2001) 813–818.
- [16] E. Liepinsh, G. Otting, Proton exchange rates from amino acid side chains—implications for image contrast, *Magn. Reson. Med.* 35 (1996) 30–42.
- [17] R. Olechnowicz, W. Masierak, J. Bodurka, A. Gutsze,  $^1\text{H}$  nmr relaxation measurements in highly concentrated water protein solutions, *Magn. Reson. Chem.* 37 (1999) S147–S149.
- [18] B.P. Hills, S.F. Takacs, P.S. Belton, The effects of proteins on the proton N.M.R. Transverse relaxation times of water—i. Native bovine serum albumin, *Mol. Phys.: Int. J. Interface Chem. Phys.* 67 (1989) 903–918.
- [19] M.S. van der Knaap, J. Valk Chapter 1, Myelin and White Matter, third ed., *Magnetic Resonance of Myelination and Myelin Disorders*, Springer, New York, 2005.
- [20] R. Ravel Chapter 19, Cerebrospinal Fluid Examination and Neurologic Disorders, sixth ed., *Clinical Laboratory Medicine: Clinical Application of Laboratory Data*, Elsevier Health Sciences, 1994.
- [21] A. Shimizu, M. Ikeguchi, S. Sugai, Appropriateness of DSS and TSP as internal references for  $^1\text{H}$  NMR studies of molten globule proteins in aqueous media, *J. Biomol. NMR* 4 (1994) 859–862.
- [22] S.C. Chu, Y. Xu, J.A. Balschi, C.S. Springer, Bulk magnetic susceptibility shifts in nmr studies of compartmentalized samples: use of paramagnetic reagents, *Magn. Reson. Med.* 13 (1990) 239–262.
- [23] G.L. Bretthorst, *Bayesian Spectrum Analysis and Parameter Estimation*, Springer-Verlag, Berlin, 1988.
- [24] J.C. Hindman, Proton resonance shift of water in the gas and liquid states, *J. Chem. Phys.* 44 (1966) 4582–4592.

- [25] R.C. Weast, M.C. Astle, *Crc handbook of chemistry and physics*, CRC Press, Cleveland, Ohio, 1981–1982.
- [26] C.K. Woodward, L.M. Ellis, A. Rosenberg, Solvent accessibility in folded proteins. Studies of hydrogen exchange in trypsin, *J. Biol. Chem.* 250 (1975) 432–439.
- [27] P.A. Srere, Macromolecular interactions: tracing the roots, *Trends Biochem. Sci.* 25 (2000) 150–153.
- [28] K. Kiyota, Soluble protein fraction of the brain tissue in relation to maturation of the brain, *Folia Psychiatr. Neurol. Jpn.* 13 (1959) 15–22.
- [29] F.O. Schmitt, Fibrous proteins–neuronal organelles, *Proc. Natl. Acad. Sci. USA* 60 (1968) 1092–1101.
- [30] K. Mizuno, S. Imafuji, T. Fujiwara, T. Ohta, Y. Tamiya, Hydration of the CH groups in 1, 4-dioxane probed by NMR and IR: contribution of blue-shifting CH–OH<sub>2</sub> hydrogen bonds, *J. Phys. Chem. B* 107 (2003) 3972–3978.
- [31] H. Chick, C.J. Martin, The density and solution volume of some proteins, *Biochem. J.* 7 (1913) 92–96.
- [32] J. Gallier, P. Rivet, J. deCertaïnes, 1H- and 2H-NMR study of bovine serum albumin solutions, *Biochim. Biophys. Acta (BBA)–Protein Struct. Mol. Enzymol.* 915 (1987) 1–18.
- [33] M. Cerdonio, S. Morante, D. Torresani, S. Vitale, A. DeYoung, R.W. Noble, Reexamination of the evidence for paramagnetism in oxy- and carbonmonoxyhemoglobins, *Proc. Natl. Acad. Sci. USA* 82 (1985) 102–103.
- [34] A.A. Spector, K. John, J.E. Fletcher, Binding of long-chain fatty acids to bovine serum albumin, *J. Lipid Res.* 10 (1969) 56–67.
- [35] D.P. Cistola, D.M. Small, J.A. Hamilton, Carbon 13 NMR studies of saturated fatty acids bound to bovine serum albumin. I. The filling of individual fatty acid binding sites, *J. Biol. Chem.* 262 (1987) 10971–10979.